



Electronic Supplementary Information (ESI)

Synthesis of conjugated segments-based cyclic polymers for direct imaging of cyclic molecular topology

Cuihong Ma,^a Ying Quan,^a Ruyi Sun,^a Wei Song,^{*b} Xiaojuan Liao^{}^{*a} and Meiran Xie^{}^{*a}

^a School of Chemistry and Molecular Engineering, East China Normal University, Shanghai 200241, China. E-mails: xjliao@chem.ecnu.edu.cn, mrxie@chem.ecnu.edu.cn

^b Department of Polymer and Composite Material, School of Materials Engineering, Yancheng Institute of Technology, Yancheng 224051, China. E-mail: sw121092@ycit.cn

Experimental

Materials and methods

All solvents were purchased from Sinopharm. Co. Ltd., and were purified by the standard procedures before use otherwise noted. All reagents were purchased from Energy Chemical and Sigma-Aldrich. Co. Ltd., and were used as received without further purification otherwise denoted. Bis(4-methoxyl-1,6-heptadiyne)-2,3,6,7-tetrachloroperylene bisimide (**BHPI**),¹ 2-(ethyl)hexyl ester-1,6-heptadiyne (**EHD**),² [1,3-bis(2,4,6-trimethylphenyl)-4,5-dihydroimidazol-2-ylidene][bis(3-bromopyridine)]benzylidene ruthenium dichloride (**Ru-III**),³ and *endo*-N-(4-hydroxyphenyl)-norbornene-dicarboximide (**NDI**)^{1,4} were prepared according to the previous procedures. 1-(3-Dimethylaminopropyl)-3-ethylcarbodiimide hydrochloride (EDCI·HCl), 4-dimethylaminopyridine (DMAP) and K₂CO₃ (99%) were purchased from Shanghai Chemical Reagents Company. 3,5-Dichloropyridine and 11-bromo-1-undecanol were purchased from Sigma-Aldrich. 1,3,6,8-Tetra(4-carboxylphenyl) pyrene was purchased from Yanshen Technology Co., Ltd. All reactions were performed under dry nitrogen atmosphere using standard Schlenk-line technique.

¹H and ¹³C NMR spectra were recorded using a Bruker 600 or 500 MHz spectrometer in CDCl₃. Gel permeation chromatography (GPC) analyses were performed on a Waters 1515 instrument equipped with a guard column MIXED 7.5×50 mm PL column and two MIXED-C 7.5×300 columns and a differential refractive index detector using THF (HPLC grade) as the eluent at 35 °C with a flow rate of 1 mL min⁻¹. The number-average molecular weight (*M_n*) and molecular weight distribution (*D*=*M_w*/*M_n*) were measured by GPC coupled with a Wyatt DAWAN 8+ light scattering (LS) detector. UV-vis spectra were performed on a UV-1800 spectrometer double beam spectrophotometer in 1.0 cm length quartz cell. ATR-IR spectra were recorded on Thermo Scientific Fourier Transorm Infrared spectrometer. Dynamic light scattering (DLS) was recorded using a Malvern Zetasizer Nano-ZS light scattering apparatus (Malvern Instruments, U.K.) with a He-Ne laser (633 nm, 4 m W), all samples were filtered with syringe filters (0.22 μ m pore size,) prior to the measurements, and all data were averaged over three time measurements. Thermal gravimetric analysis (TGA) was performed by an SDT851e/SF/1100 °C TGA instrument under nitrogen flow at a heating rate of 10 °C min⁻¹ from 25 to 800 °C. Differential scanning calorimeter (DSC) was carried out with Q2000 DSC system in nitrogen atmosphere. An indium standard was used for temperature and enthalpy calibrations. All the samples were first heated from 25 to 200 °C at a rate of 30 °C min⁻¹

and held at this temperature for 3 min to eliminate the thermal history, then they were cooled to 25 °C and heated again from 25 to 200 °C at a heating or cooling rate of 10 °C min⁻¹. Transmission electron microscopy (TEM) images were recorded on the JEOL JEM2100F. Samples for TEM measurements were prepared by drop casting the highly diluted THF solution (0.001 mg mL⁻¹) of polymer onto the surface of pure carbon film on copper screen. Cyclic voltammetry (CV) was performed at 25 °C with an Autolab PGSTAT12 potentiostat equipped with an electrochemical cell with three electrodes. Ag/AgCl was used as the reference electrode, platinum electrode as counter electrode and a glassy carbon electrode was used as working electrode. Then a 0.1 M CH₃CN solution of Bu₄NPF₆ was used as the supporting electrolyte, and Fc⁺/Fc was used as the reference. The solution of the material to be tested was dropped on the working electrode and dried to form a film for testing. The E_{HOMO} , E_{g} , and E_{LUMO} were calculated as refer to the eqs 1, 2, and 3.

$$E_{\text{LUMO}} = -(E_{\text{onset}}^{\text{red}} + 4.4) \text{ eV} \quad (1)$$

$$E_{\text{g}} = 1240/\lambda_{\text{edg}} \quad (2)$$

$$E_{\text{HOMO}} = E_{\text{LUMO}} - E_{\text{g}} \quad (3)$$

Synthesis of tetrafunctional monomer TNBP

Synthesis of NDI-OH

Under a nitrogen atmosphere, **NDI** (10.0 g, 39.25 mmol) and K₂CO₃ (16.1 g, 117.75 mmol) were dissolved in dry DMF (200 mL), 11-bromo-1-undecanol (11.8 g, 47.01 mmol) was then added after 10 min, and the reaction mixture was stirred at 100 °C for 8 h. Upon cooling, the reaction mixture was dropped into an excess of water (2 L), filtered, and a white solid **NDI-OH** was obtained (15.5 g, 93%). ¹H NMR (500 MHz, DMSO-*d*₆, ppm) δ 6.97 (s, 4H, aromatic), 6.20 (s, 2H, CH=CH), 4.32 (s, 1H, CH₂OH), 3.96 (s, 2H, Ph-OCH₂), 3.45 (s, 2H, CH₂OH), 1.70-1.25 (m, 23H, CH=CHCH + CH=CHCHCHCO + CH=CHCHCH + 9CH₂). ¹³C NMR (125 MHz, DMSO-*d*₆, ppm): δ 177.52, 158.96, 134.98, 128.68, 125.15, 114.82, 68.14 (s), 67.98, 61.29, 52.16, 45.52, 33.33, 29.42, 25.82.

Synthesis of TNBP

Under a nitrogen atmosphere, to a solution of 1,3,6,8-tetra(4-carboxylphenyl) pyrene (2.4 g, 3.50 mmol) in 180 mL of anhydrous CH₂Cl₂, **NDI-OH** (12.0 g, 28.02 mmol) and DMAP (1.71 g, 2.81 mmol) were added under stirring for 30 min, a large amount of 1,3,6,8-tetra(4-carboxylphenyl) pyrene was not dissolved, and then EDCI•HCl (5.3 g, 16.8

mmol) was added to the mixture and stirred at room temperature for 4 days. After that, 1,3,6,8-tetra(4-carboxylphenyl) pyrene was almost completely dissolved, and the solution appeared light fluorescent blue. The solvent was removed under reduced pressure. The solid was purified by column chromatography on silica gel using PE/EA=2:1 as eluent to afford 1,3,6,8-tetra(4-(N-4-phenoxy undecyl norbornene dicarboximide) benzoate) pyrene, **TNBP**, (3.5 g, 44%) as a fluorescent green powder. ^1H NMR (500 MHz, CDCl_3 , ppm): δ 8.24-8.22 (d, 8H, aromatic), 8.15 (s, 4H, aromatic), 8.0 (s, 2H, aromatic), 7.75-7.74 (d, 8H, aromatic), 7.01-7.00 (m, 8H, aromatic), 6.91-6.89 (m, 8H, aromatic), 6.24 (t, 8H, $\text{CH}=\text{CH}$), 4.40-4.37 (t, 8H, CO_2CH_2), 3.94-3.91 (t, 8H, OCH_2), 3.48 (s, 8H, $\text{CH}=\text{CHCH}$), 3.40-3.37 (m, 8H, $\text{CH}=\text{CHCHCH}$), 1.85-1.31 (m, 60H, $9\text{CH}_2 + \text{CH}=\text{CHCH}_2$). ^{13}C NMR (125 MHz, CDCl_3 , ppm): δ 177.52, 166.93, 159.47, 145.68, 137.02, 134.97, 131.03, 130.11, 128.72, 128.17, 124.61, 115.32, 68.58, 65.73, 52.60, 46.10, 45.84, 29.92, 29.73, 29.71, 29.53, 29.18, 26.46, 26.39. ATR-IR (cm^{-1}): 2928 ($\nu_{\text{C-H}}$), 2857 ($\nu_{\text{C-H}}$), 1704 ($\nu_{\text{C=O}}$), 1177 ($\nu_{\text{C-O}}$).

Synthesis of homopolymer PTNBP

The tetrafunctional monomer 1,3,6,8-tetra{4-[(N-4-phenoxy undecyl) norbornene imide] benzoate} pyrene (**TNBP**) (23.1 mg, 0.01 mmol) was dissolved in 19 mL of CH_2Cl_2 charged in a 100 mL Schlenk tube. In another 25 mL Schlenk tube, **Ru-III** (1.76 mg, 0.002 mmol) was dissolved in 1 mL of CH_2Cl_2 . After degassed with three freeze-vacuum-thaw cycles, the solution of **Ru-III** was then injected into 100 mL Schlenk tube via a syringe under vigorous stirring for 1 h at 30 °C. The solution was precipitated into methanol and dried under vacuum to afford homopolymer **PTNBP** as a light green solid (21.2 mg, 92%). GPC: $M_n=4.2 \text{ kg mol}^{-1}$, $M_w=10.0 \text{ kg mol}^{-1}$, $D=1.26$. ^1H NMR (500 MHz, CDCl_3): δ 8.23 (br, CO_2CCH), 8.14-8.13 (br, pyrene), 8.01-7.98 (br, pyrene), 7.75-7.74 (br, pyrene), 7.12-6.97 (br, NCCH), 6.00-5.65 (br, CH on PNBE backbone), 4.38 (s, CO_2CH_2), 3.94-3.86 (br, Ph-OCH_2), 3.33 (s, $=\text{CHCH}$), 2.96 (s, $=\text{CHCHCH}$), 1.80-1.26 (br, $=\text{CHCHCH}_2 + \text{Ph-OCH}_2(\text{CH}_2)_9$).

General procedure for metathesis cyclopolymerization

Typically, the **Ru-III** initiated successive metathesis cyclopolymerization (MCP) of di- and mono-functional 1,6-heptadiyne derivatives were carried out in a Schlenk tube under dry nitrogen atmosphere at -5 °C in CH_2Cl_2 for a preset time. After confirmed the monomer conversion by TLC, ethyl vinyl ether (0.2 mL) was added to the reaction mixture and stirred for further 2 h, and the mixture was concentrated and poured into an excess of the mixed solvent of methanol and acetone (v/v=3:1). The polymer was washed with mixed solvent, and dried in a vacuum oven at 30 °C to a constant weight.

Successive MCP of BHPI and EHD for synthesis of linear polymer

A 100 mL of Schlenk tube was charged with bifunctional monomer **BHPI** (69.0 mg, 0.06 mmol) dissolved in 29 mL of CH₂Cl₂. Monofunctional monomer **EHD** (148.8 mg, 0.6 mmol) dissolved in 1 mL of CH₂Cl₂ in 25 mL of Schlenk tubes. **Ru-III** (5.3 mg, 6.0 μmol) and 3,5-dichloropyridine (8.8 mg, 0.06 mmol) were dissolved in 1 mL of CH₂Cl₂ in 25 mL of Schlenk tubes. After degassed with three freeze-vacuum-thaw cycles, the solution of **Ru-III** and 3,5-dichloropyridine were injected into the **BHPI** solution via a syringe under vigorous stirring at -5 °C for 30 min, and then **EHD** was injected into the reaction solution and stirred for further 2 h, affording *l*-**PBHPI**₂₀-(*b*-**PEHD**₁₀₀)₂ (167.6 mg, 77%). GPC: $M_{n,t}$ =40.4 kDa, D =1.55. ¹H NMR (600 MHz, CDCl₃): δ 8.66-8.58 (br, pery), 6.67-6.27 (br, *trans*-CH on PA backbone), 4.20-4.03 (br, CCCH₂CHCH₂ + PBI-CH₂ + CO₂CH₂), 3.20-2.27 (br, CCCH₂ + CCCH₂CH + CH₂CO₂CH₂), 1.72-1.30 (PBI-CH₂(CH₂)₉) + CH₃(CH₂)₃CH + CH₃CH₂CH), 0.92-0.89 (br, CH₃CH₂CH₂CH₂CH + CH₃CH₂CH). ¹³C NMR (150 MHz, CDCl₃): δ 175.72, 162.09, 138.15, 135.14, 132.83, 128.39, 123.11, 67.33, 40.33, 38.67, 37.15, 34.15, 30.36, 28.82, 23.83, 22.93, 14.02, 10.95.

Successive MCP of BHPI, EHD and BHPI for synthesis of monocyclic polymers

Two sets of bifunctional monomers **BHPI** (34.5 mg, 0.03 mmol) were dissolved in 59 mL and 1 mL of CH₂Cl₂ in 250 mL and 25 mL of Schlenk tubes, separately. **Ru-III** (5.3 mg, 6.0 μmol) and 3,5-dichloropyridine (8.8 mg, 0.06 mmol) were dissolved in 1 mL of CH₂Cl₂ in 25 mL of Schlenk tubes, as well as monofunctional monomer **EHD** (148.8 mg, 0.6 mmol) were dissolved in 1 mL of CH₂Cl₂ in 25 mL of Schlenk tubes. After degassed with three freeze-vacuum-thaw cycles, the solution of **Ru-III** and 3,5-dichloropyridine were injected into the **BHPI** solution in a 100 mL of Schlenk tube via a syringe under vigorous stirring at -5 °C for 30 min, and then **EHD** was injected into the reaction solution and stirred for further 30 min. At last, the **BHPI** solution was injected into the reaction mixture and stirred for another 2 h, affording the monocyclic polymer *c*-[**PBHPI**₁₀-(*b*-**PEHD**₁₀₀)₂-*b*-**PBHPI**₁₀] (174.2 mg, 80%). GPC: $M_{n,c}$ =30.7 kDa, D =1.56. ¹H NMR (600 MHz, CDCl₃): δ 8.66-8.58 (br, pery), 6.67-6.28 (br, *trans*-CH on PA backbone), 4.20-4.02 (br, CCCH₂CHCH₂ + PBI-CH₂ + CO₂CH₂), 3.20-2.28 (br, CCCH₂ + CCCH₂CH + CH₂CO₂CH₂), 1.71-1.30 (PBI-CH₂(CH₂)₉) + CH₃(CH₂)₃CH + CH₃CH₂CH), 0.92-0.89 (br, CH₃CH₂CH₂CH₂CH + CH₃CH₂CH). ¹³C NMR (150 MHz, CDCl₃): δ 175.67, 162.15, 138.14, 135.19, 132.88, 128.55, 123.05, 67.33, 40.34, 38.67, 37.12, 34.16, 30.86, 30.36, 28.82, 23.83, 22.93, 14.01, 10.95.

Linear polymer *l*-**PBHPI**₂₀-(*b*-**PEHD**₂₀₀)₂ and monocyclic polymer *c*-[**PBHPI**₁₀-(*b*-

PEHD₂₀₀)₂-*b*-**PBHPI**₁₀] were prepared in a similar way with the above synthetic routes. The characterization data for the above polymers were listed in Table 1.

Tandem ROMP-MCP reaction to synthesize linear polymers

A 50 mL of Schlenk tube was charged with tetrafunctional monomer 1,3,6,8-tetra(4-(N-4-phenoxy undecyl norbornene dicarboximide) benzoate) pyrene (**TNBP**) (17.3 mg, 7.5 μ mol) dissolved in 14 mL of CH₂Cl₂. Bifunctional monomer **BHPI** (34.5 mg, 0.03 mmol) and 3,5-dichloropyridine (8.8 mg, 0.06 mmol) were dissolved in 1 mL of CH₂Cl₂ in 25 mL of Schlenk tubes. As well as monofunctional monomer **EHD** (148.8 mg, 0.6 mmol) and 3,5-dichloropyridine (8.8 mg, 0.06 mmol) were dissolved in 1 mL of CH₂Cl₂ in two 25 mL of Schlenk tubes. **Ru-III** (5.3 mg, 6.0 μ mol) was dissolved in 1 mL of CH₂Cl₂ in two 25 mL of Schlenk tubes. After degassed with three freeze-vacuum-thaw cycles, **Ru-III** solution was injected into the **TNBP** solution in a 50 mL of Schlenk tube via a syringe under vigorous stirring at 30 °C for 60 min, and then the solution of **BHPI** and 3,5-dichloropyridine was injected into the reaction solution at -5 °C and stirred for further 30 min. At last, the **EHD** solution was injected into the reaction mixture and stirred for another 2 h, affording the linear copolymer *l*-**PTNBP**₅-(*b*-**PBHPI**₁₀)₂-(*b*-**PEHD**₁₀₀)₄ (160.4 mg, 80%). GPC: $M_{n,t}$ =83.2 kDa, D =1.58. ¹H NMR (500 MHz, CDCl₃, 25 °C): δ 8.67-8.65 (br, pery), 8.21-7.99 (br, pyrene + pyrene-CCHCH), 7.73 (s, pyrene-CCHCH), 7.08-6.27 (br, *trans*-CH on PA backbone + NCCHCH + NCCHCH), 4.37-4.02 (br, CCCH₂CHCH₂ + pery-CH₂ + CO₂CH₂ + pyrene-Ph-CO₂CH₂ + N-Ph-OCH₂), 3.20-2.79 (br, CCCH₂ + CCCH₂CH + CO₂CH₂ + NCOCHCH + NCOCHCH), 1.72-1.27 (br, pyrene-CO₂CH₂(CH₂)₉ + CO₂CH₂(CH₂)₉ + CH₃(CH₂)₃CHCH₂CH₃ + CCCHCH₂), 0.92-0.88 (br, CO₂CH₂CH(CH₂)₃CH₃ + CO₂CH₂CHCH₂CH₃).

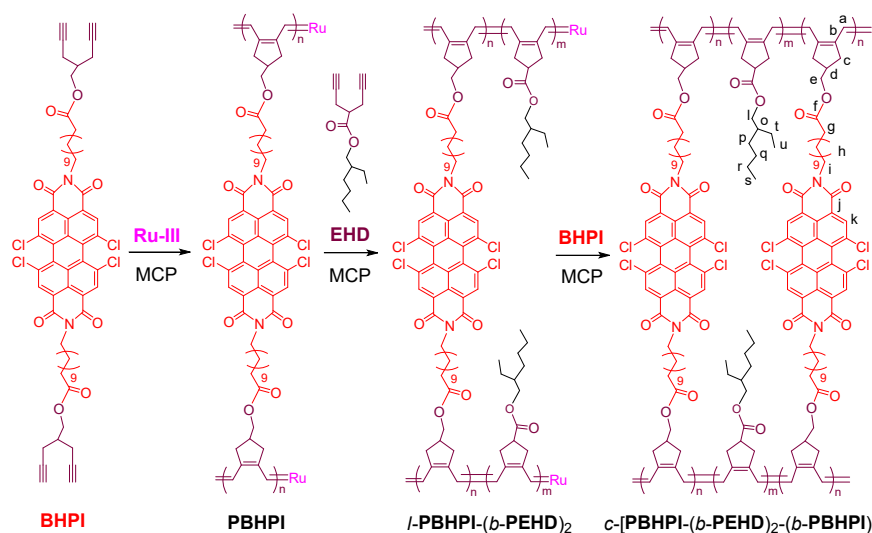
Tandem ROMP-MCP to synthesize bicyclic polymers

A 50 mL of Schlenk tube was charged with tetrafunctional monomer **TNBP** (17.3 mg, 7.5 μ mol) dissolved in 14 mL of CH₂Cl₂. Bifunctional monomer **BHPI** (34.5 mg, 0.03 mmol) and 3,5-dichloropyridine (8.8 mg, 0.06 mmol) were dissolved in 1 mL of CH₂Cl₂ in 25 mL of Schlenk tubes. As well as monofunctional monomer **EHD** (148.8 mg, 0.6 mmol) and 3,5-dichloropyridine (8.8 mg, 0.06 mmol) were dissolved in 1 mL of CH₂Cl₂ in two 25 mL of Schlenk tubes. **Ru-III** (5.3 mg, 6.0 μ mol) was dissolved in 1 mL of CH₂Cl₂ in two 25 mL of Schlenk tubes. After degassed with three freeze-vacuum-thaw cycles, **Ru-III** solution was injected into the **TNBP** solution in a 50 mL of Schlenk tube via a syringe under vigorous stirring at 30 °C for 60 min, and then the solution of **EHD** and 3,5-dichloropyridine was injected into the reaction solution at -5 °C and stirred for further 30

min. At last, the **BHPI** solution was injected into the reaction mixture and stirred for another 2 h, affording the bicyclic polymer $c\text{-}[\text{PTNBP}_5\text{-(}b\text{-PEHD}_{100})_4\text{-(}b\text{-PBHPI}_{10})_2]$ (164.4 mg, 82%). GPC: $M_{n,c}$ =69.5 kDa, D =1.56. ^1H NMR (500 MHz, CDCl_3 , 25 °C): δ 8.67-8.62 (br, pery), 8.21-7.99 (br, pyrene + pyrene-CCHCH), 7.73 (s, pyrene-CCHCH), 7.09-6.14 (br, *trans*-CH on PA backbone + NCCHCH + NCCHCH), 4.37-4.02 (br, CCCH₂CHCH₂ + pery-CH₂ + CO₂CH₂ + pyrene-Ph-CO₂CH₂ + N-Ph-OCH₂), 3.21-2.80 (br, CCCH₂ + CCCH₂CH + CO₂CH₂ + NCOCHCH + NCOCHCH), 1.65-1.27 (br, pyrene-CO₂CH₂(CH₂)₉ + CO₂CH₂(CH₂)₉ + CH₃(CH₂)₃CHCH₂CH₃ + CCCHCH₂), 0.92-0.89 (br, CO₂CH₂CH(CH₂)₃CH₃ + CO₂CH₂CHCH₂CH₃).

Linear polymer $l\text{-PTNBP}_5\text{-(}b\text{-PBHPI}_{10})_2\text{-(}b\text{-PEHD}_{200})_4$ and bicyclic polymer $c\text{-}[\text{PTNBP}_5\text{-(}b\text{-PEHD}_{200})_4\text{-(}b\text{-PBHPI}_{10})_2]$ was synthesized in a similar way.

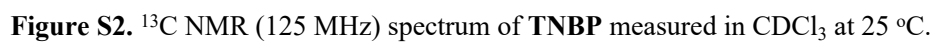
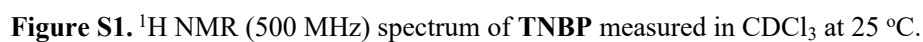
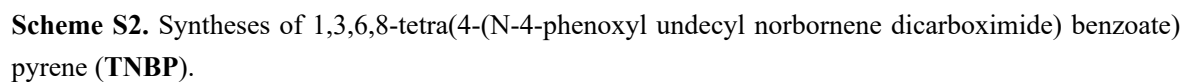
Results and discussion



Scheme S1. Synthesis of monocyclic polymers by MCP-based blocking-cyclization process.

Synthesis and characterization of tetrafunctional monomer TNBP

A tetrafunctional norbornene monomer **TNBP** was prepared via conventional reactions (Scheme S2), and the experimental and characterization details were described in Supporting Information and Figures S1-S3. From ^1H NMR spectrum (Figure S1), the ratios of the integral area of protons H_a at 6.24-6.23 ppm to those of protons H_i at 4.40-4.37 ppm and protons H_m at 8.15 ppm were calculated to be 8:8:4, which matched well with the theoretical values, indicating the successful preparation of monomer **TNBP**.



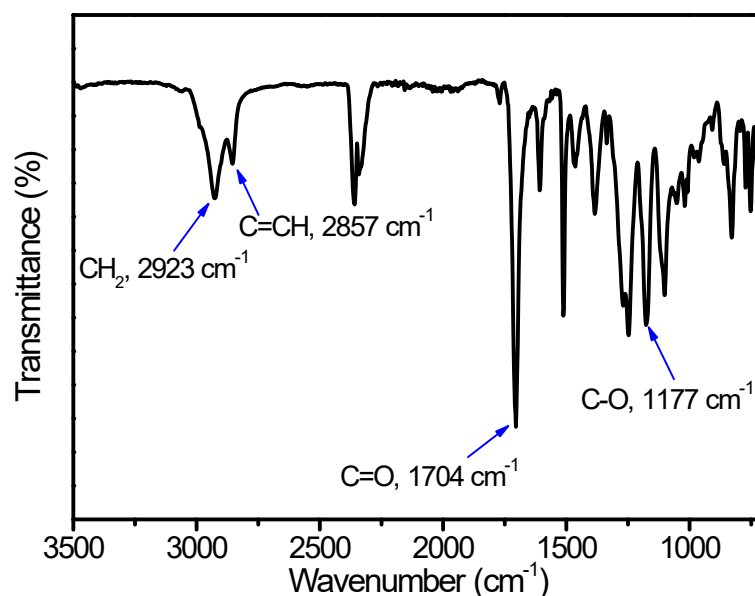


Figure S3. ATR-IR spectrum of **TNBP**.

Synthesis and characterization of homopolymer **PTNBP**

ROMP of tetrafunctional **TNBP** was attempted under the feed ratio ($[\text{TNBP}]/[\text{Cat}]$) of 10:4 at the initial monomer concentration of $3 \times 10^{-4} \text{ mol L}^{-1}$ for 0.5 h (entry 1, Table S1). Unfortunately, it was found that a large amount of **TNBP** remained through TLC analysis, likely due to the low concentration and relatively more loading of **TNBP**. By reducing the feed ratio of $[\text{TNBP}]/[\text{Cat}]$ to 5:4, increasing monomer concentration to $5 \times 10^{-4} \text{ mol L}^{-1}$, and extending polymerization time to 1 h, **TNBP** consumed completely to generating homopolymer **PTNBP**₅ in a high yield (entry 2, Table S1), which behaved the number-average molecular weight (M_n) of 4.2 kg mol^{-1} and narrow polydispersity (D) of 1.26 by gel permeation chromatography (GPC) analysis (Figure S4b). Furthermore, the absolute molecular weight (M_w) of **PTNBP**_n ($M_w=10.0 \text{ kg mol}^{-1}$) was in good agreement with the theoretical value of 11.5 kg mol^{-1} , suggesting the successful preparation of homopolymer **PTNBP**₅. As expected, the olefinic protons on the norbornenyl ring at 6.23 ppm (Figure S1) disappeared, and a new broad peak of olefinic protons (H_a) on the backbone was located at 6.00-5.65 ppm in ^1H NMR spectrum (Figure S4a). In addition, the ladder conformation of **PTNBP**₅ was observed from the TEM image (Figures S4c-S4e), and the black lines aligned parallel to each other to form the ladder strips, meanwhile, the average spacing of each strip was nearly 0.35 nm, meaning that there was a strong π - π interaction between the pyrenyl moieties. Also, the relative selected area electron diffraction (SAED) pattern of **PTNBP**₅ (Figure S4f) exhibited regular diffraction spots,¹ which provided

another evidence for confirming the ladder structure of this homopolymer. As a result, this short ladderphane **PTNBP**₅ would play a key role as the starting motif in preparing bicyclic polymer by blocking-cyclization technique, in which another ladderphane **PBNP**₅ was chosen as a cyclizing unit to ensure the cyclizing efficiency and high purity of bicyclic polymer.

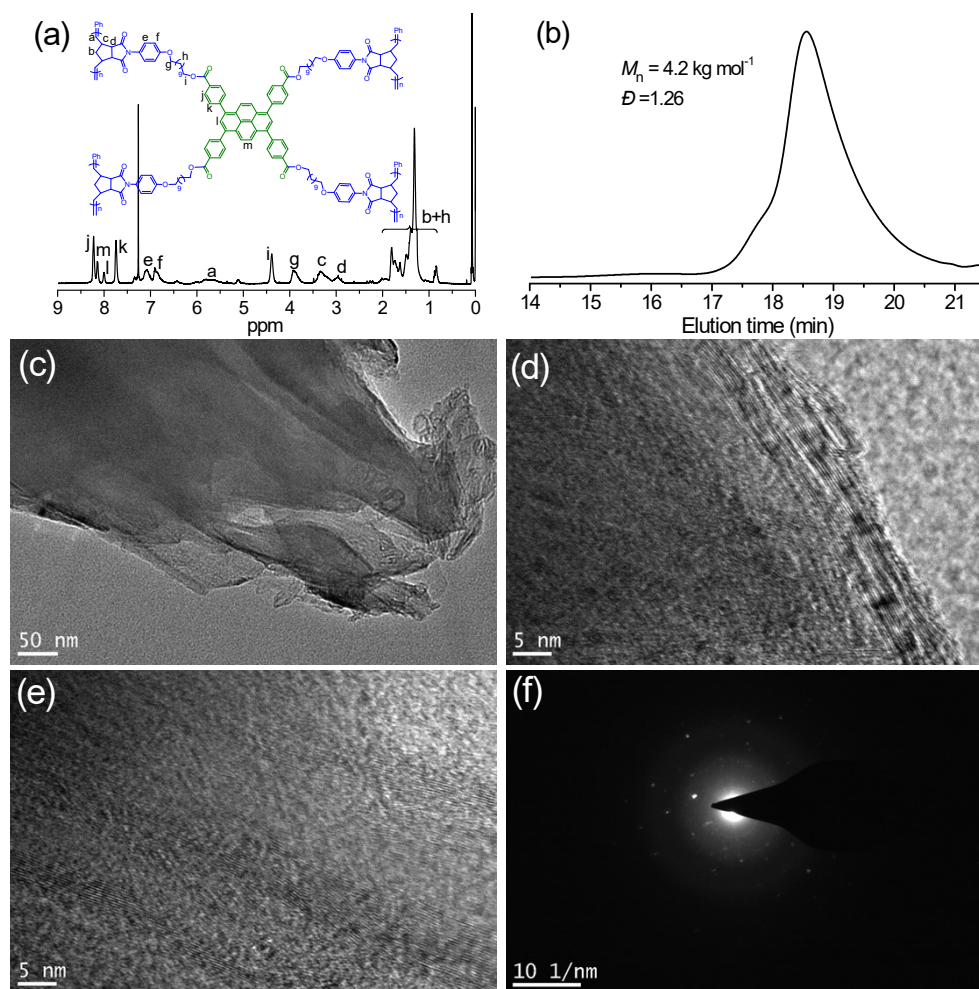


Figure S4. ¹H NMR (500 MHz) spectrum measured in CDCl₃ at 25 °C (a), GPC trace (b), TEM images (c-e), and the corresponding SAED pattern of homopolymer ladderphane **PTNBP**₅ (f).

Table S1 Characteristics for homopolymer^a

Entry	Polymer	[TNBP]:[Cat] ^b	t (h)	M_n^c (kg mol ⁻¹)	\bar{D}^c	Yield (%)
1 ^d	PTNBP ₁₀	10:4	0.5	/	/	53.0
2 ^e	PTNBP ₅	5:4	1.0	4.2	1.26	92.0

^aPolymerization conditions: using **Ru-III** as catalyst, CH₂Cl₂ as solvent, temperature=30 °C. Polymerization time: 0.5 h for entry 1 and 1 h for entry 2.

^bThe molar feeding ratio of tetrafunctional monomer **TNBP** to catalyst.

^cDetermined by GPC in THF relative to monodispersed polystyrene standards.

^d[TNBP]₀ = 3×10⁻⁴ mol L⁻¹.

^e[TNBP]₀ = 5×10⁻⁴ mol L⁻¹.

Synthesis and characterization of cyclic copolymers

As displayed in Figures S6a and S6b, ^1H NMR spectra of these two polymers possessing the same components showed the complete disappearance of signal peak at 2.01-2.00 ppm ascribed to the alkyne protons of $\text{CH}\equiv\text{C}-$ in **EHD** and **BHPI**, while a new broad signal peak at 6.67-6.27 ppm attributed to the conjugated protons (H_a) of $-\text{CH}=\text{CH}-$ bonds on PA backbone was clearly observed, and also the signals of aromatic protons (H_k) on perylene bisimide linker of **BHPI** at 8.66-8.60 ppm and those of terminal methyl protons ($\text{H}_{s,u}$) on **EHD** at 0.92-0.89 ppm were found, meaning the successful polymerization. Meanwhile, by integrating the peak signals, the ratios of **BHPI/EHD** for linear and cyclic polymers were 20:284 and 20:290, respectively, which were similar with each other due to the same feed ratio. However, it was smaller than the theoretical block ratios of 20:400, because it was difficult to obtain polymers with much longer PA skeleton when the molecular chain grows to a certain extent. Moreover, the signals of alkyne carbon $\text{CH}\equiv\text{C}-$ and methylene carbon on 1,6-heptadiyne at 80.31, 70.61, and 19.9 ppm disappeared entirely after MCP, while new peak appeared at 138.25 ppm (Figures S6c and S6d), which were attributed to the carbon signals of conjugated double bond on the five-membered ring, indicating that the effective cyclization reaction was completed successfully. Characterization by ATR-IR provided further evidence for the successful synthesis of linear *l*-**PBHPI**₂₀-(*b*-**PEHD**₂₀₀)₂ and monocyclic *c*-[**PBHPI**₁₀-(*b*-**PEHD**₂₀₀)₂-(*b*-**PBHPI**₁₀)] (Figures S7c and S7d). The peaks at 3310 cm^{-1} ($\text{HC}\equiv$ stretching vibration) and 2118 cm^{-1} ($\text{C}\equiv\text{C}$ stretching vibration) in ATR-IR spectra of monomers **EHD** and **BHPI** (Figures S7a and S7b) disappeared completely, in other words, there was no monomer residual in polymer. Then, linear *l*-[**PTNBP**₅-(*b*-**PBHPI**₁₀)₂-(*b*-**PEHD**_m)₄] and bicyclic *c*-[**PTNBP**₅-(*b*-**PEHD**_m)₄-(*b*-**PBHPI**₁₀)₂] ($m=100, 200$) (entries 5-8, Table S2) were tried to synthesize by tandem ROMP-MCP based on blocking-cyclization technique (Scheme S3), which was realized by replacing the starting monomer **BHPI** with tetrafunctional monomer **TNBP**. Comparing bicyclic polymers with linear counterparts, the actual ratios of **PTNBP/PEHD/PBHPI** for the above two pairs of polymers were calculated to be 5:328:20, 5:336:20, 5:589:20, and 5:570:20 by ^1H NMR analysis (Figures S8 and S9), separately. IR spectrometry also suggested the successful synthesis of polymers, depicted as the disappearance of $\text{H}\equiv\text{C}-$

(3310 cm⁻¹) and C≡C (2118 cm⁻¹) stretching vibrations (Figure S10).

Table S2 Synthetic data for linear and cyclic polymers^a

Entry	Polymer	T (°C)	[TNBP]:[BHPI]:[EHD]: [BHPI]:[Cat] ^b	[TNBP]:[BHPI]: [EHD] ^c	<i>M_n</i> ^d (kDa)	<i>Đ</i> ^d	Conv ^e (%)
1 ^f	<i>l</i> -PBHPI ₂₀ -(<i>b</i> -PEHD ₁₀₀) ₂	-5	0:20:200:0:2	0:20:160	40.4	1.55	80
2 ^g	<i>c</i> -[PBHPI ₁₀ -(<i>b</i> -PEHD ₁₀₀) ₂ -(<i>b</i> -PBHPI ₁₀)]	-5	0:10:200:10:2	0:20:163	30.7	1.56	82
3 ^f	<i>l</i> -PBHPI ₂₀ -(<i>b</i> -PEHD ₂₀₀) ₂	-5	0:20:400:0:2	0:20:284	73.3	1.57	71
4 ^g	<i>c</i> -[PBHPI ₁₀ -(<i>b</i> -PEHD ₂₀₀) ₂ -(<i>b</i> -PBHPI ₁₀)]	-5	0:10:400:10:2	0:20:290	56.1	1.56	73
5 ^f	<i>l</i> -PTNBP ₅ -(<i>b</i> -PBHPI ₁₀) ₂ -(<i>b</i> -PEHD ₁₀₀) ₄	30, -5	5:20:400:0:4	5:20:328	83.2	1.58	82
6 ^g	<i>c</i> -[PTNBP ₅ -(<i>b</i> -PEHD ₁₀₀) ₄ -(<i>b</i> -PBHPI ₁₀) ₂]	30, -5	5:0:400:20:4	5:20:336	69.5	1.56	84
7 ^f	<i>l</i> -PTNBP ₅ -(<i>b</i> -PBHPI ₁₀) ₂ -(<i>b</i> -PEHD ₂₀₀) ₄	30, -5	5:20:800:0:4	5:20:589	125.7	1.59	74
8 ^g	<i>c</i> -[PTNBP ₅ -(<i>b</i> -PEHD ₂₀₀) ₄ -(<i>b</i> -PBHPI ₁₀) ₂]	30, -5	5:0:800:20:4	5:20:570	96.1	1.57	72

^aPolymerization conditions: using **Ru-III** as catalyst, and CH₂Cl₂ as solvent. (30+120) min for entries 1 and 3, (30+30+120) min for entries 2 and 4, and (60+30+120) min for entries 5-8. 30 °C for **TNBP** of entries 5-8 and -5 °C for **EHD** and **BHPI** of entries 1-8. ^bFeed ratios of monomers to catalyst. ^cBlock ratios by ¹H NMR analysis. ^dDetermined by GPC in THF relative to monodispersed polystyrene standards. ^eCalculated by ¹H NMR analysis. ^f[BHPI]₀=2×10⁻³ mol L⁻¹ and [TNBP]₀=2×10⁻³ mol L⁻¹ refer to the initial monomer concentration. ^g[BHPI]₀=5×10⁻⁴ mol L⁻¹ and [TNBP]₀=5×10⁻⁴ mol L⁻¹ refer to the initial monomer concentration.

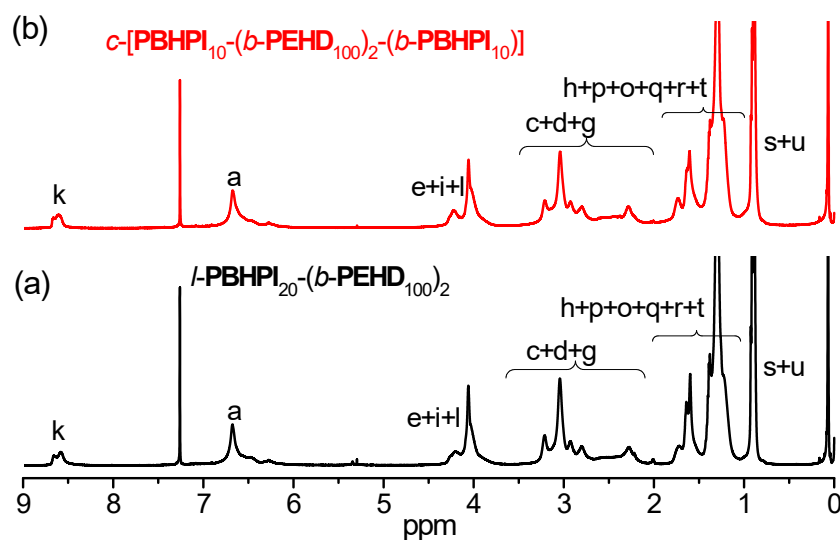


Figure S5. The ^1H NMR spectra of linear (a) and monocyclic (b) polymers in CDCl_3 .

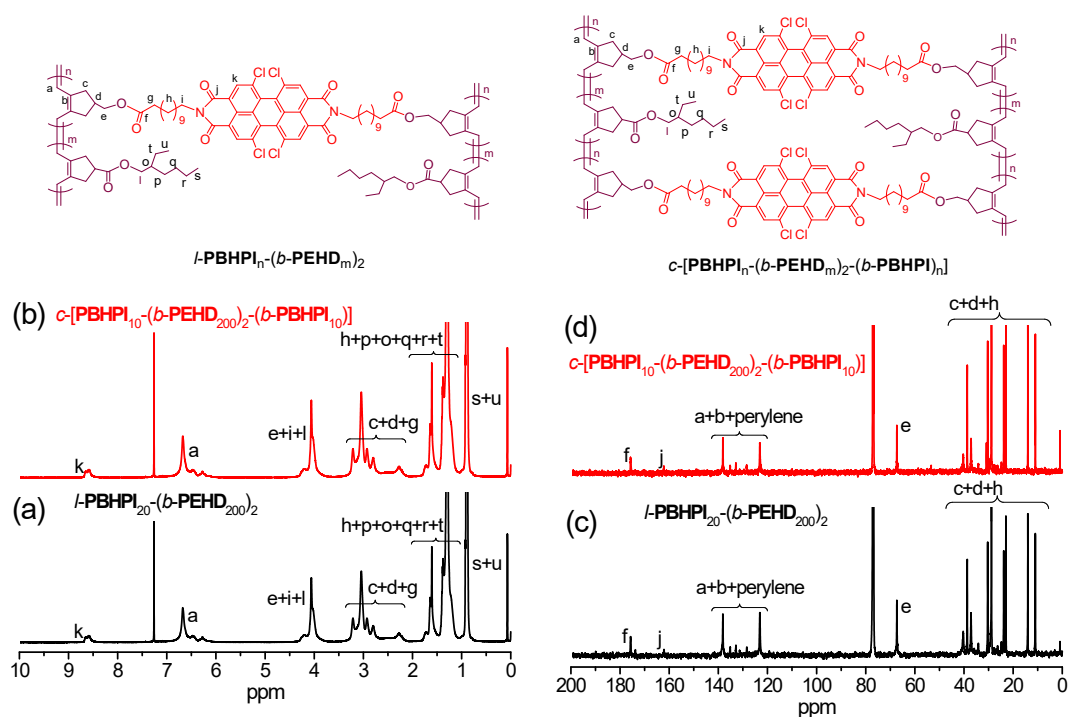


Figure S6. ^1H (a,b) and ^{13}C (c,d) NMR spectra of linear $l\text{-PBHPI}_{20}\text{-(b-PEHD}_{200})_2$ (a,c) and monocyclic $c\text{-[PBHPI}_{10}\text{-(b-PEHD}_{200})_2\text{-(b-PBHPI}_{10})]$ (b,d) in CDCl_3 .

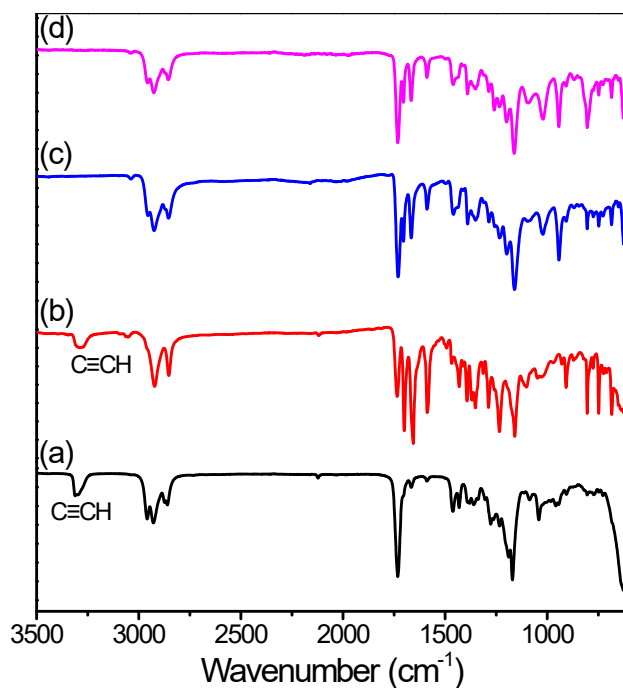


Figure S7. ATR-IR spectra of **EHD** (a), **BHPI** (b), ***l*-PBHPI₂₀-(*b*-PEHD₂₀₀)₂** (c), and monocyclic ***c*-[PBHPI₁₀-(*b*-PEHD₂₀₀)₂-(*b*-PBHPI₁₀)]** (d) measured at 25 °C.

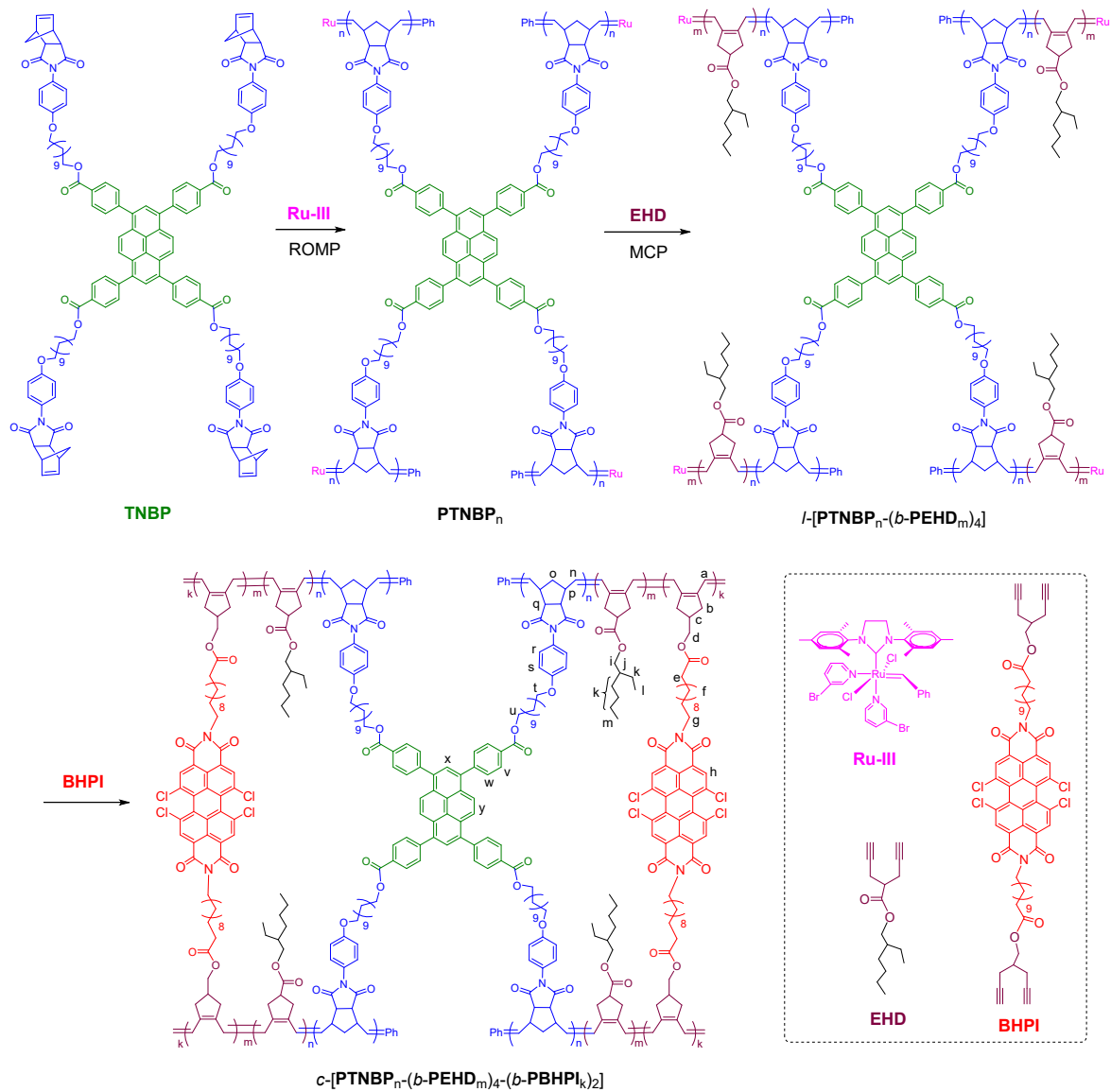
Table S3 Intrinsic viscosity data over a range of M_w for monocyclic and linear polymers, and $[\eta]_c/[\eta]_l$.

<i>l</i> -PBHPI ₂₀ -(<i>b</i> -PEHD ₂₀₀) ₂		<i>c</i> -[PBHPI ₁₀ -(<i>b</i> -PEHD ₂₀₀) ₂ -(<i>b</i> -PBHPI ₁₀)]		$[\eta]_c/[\eta]_l$
Log(M_w)	$[\eta]_l$ (mL g ⁻¹)	Log(M_w)	$[\eta]_c$ (mL g ⁻¹)	
5.05	33.2	5.05	29.5	0.88
5.1	44.1	5.1	37.8	0.85
5.2	76.2	5.2	63.4	0.83
5.3	133.8	5.3	106.8	0.80
5.4	233.3	5.4	168.5	0.72

Table S4 $\langle R_g \rangle$ values over a range of M_w for monocyclic and linear polymers, and $\langle R_g^2 \rangle_c / \langle R_g^2 \rangle_l$.

<i>l</i> -PBHPI ₂₀ -(<i>b</i> -EHD ₂₀₀) ₂		<i>c</i> -[PBHPI ₁₀ -(<i>b</i> -PEHD ₂₀₀) ₂ -(<i>b</i> -PBHPI ₁₀)]		$\langle R_g^2 \rangle_c / \langle R_g^2 \rangle_l$
M_w (Da)	$\langle R_g \rangle$ (nm)	M_w (Da)	$\langle R_g \rangle$ (nm)	
50433	16.50	50278	12.40	0.56
70359	18.45	70281	14.31	0.60
90980	20.20	90123	16.00	0.62
119978	22.69	120888	18.13	0.63
151507	25.17	150316	20.00	0.63
181252	27.38	180754	21.84	0.63

202093	29.22	201310	22.94	0.61
223400	30.55	222932	23.47	0.58
264052	33.95	262650	25.76	0.57
323086	39.59	323373	28.50	0.52
359735	42.18	359828	30.79	0.53



Scheme S3. Synthesis of bicyclic polymers by tandem ROMP-MCP process.

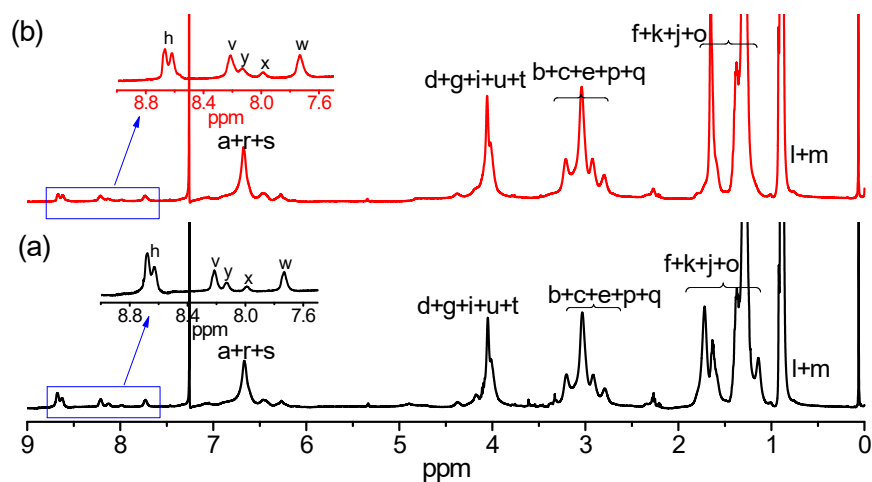


Figure S8. ^1H NMR spectra of L -[PTNBP₅-(b -PBHPI₁₀)₂-(b -PEHD₁₀₀)₄] (a) and bicyclic c -[PTNBP₅-(b -PEHD₁₀₀)₄-(b -PBHPI₁₀)₂] (b) in CDCl_3 .

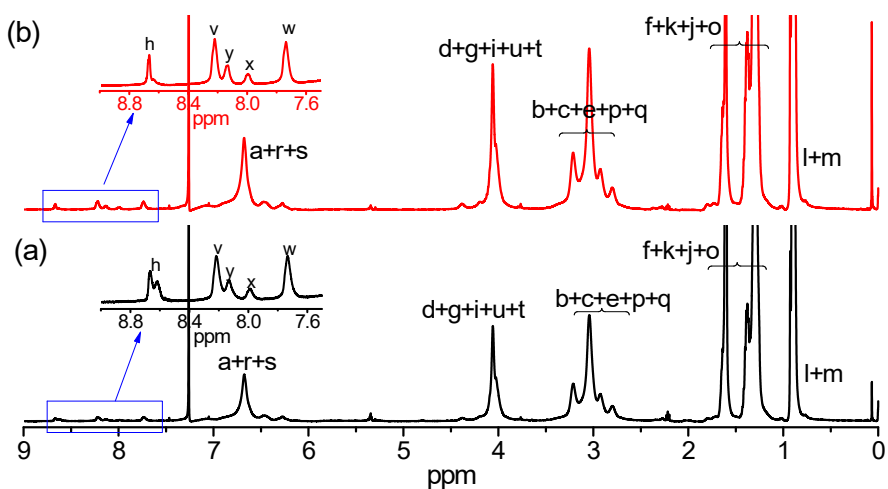


Figure S9. ^1H NMR spectra of L -[PTNBP₅-(b -PBHPI₁₀)₂-(b -PEHD₂₀₀)₄] (a) and bicyclic c -[PTNBP₅-(b -PEHD₂₀₀)₄-(b -PBHPI₁₀)₂] (b) in CDCl_3 .

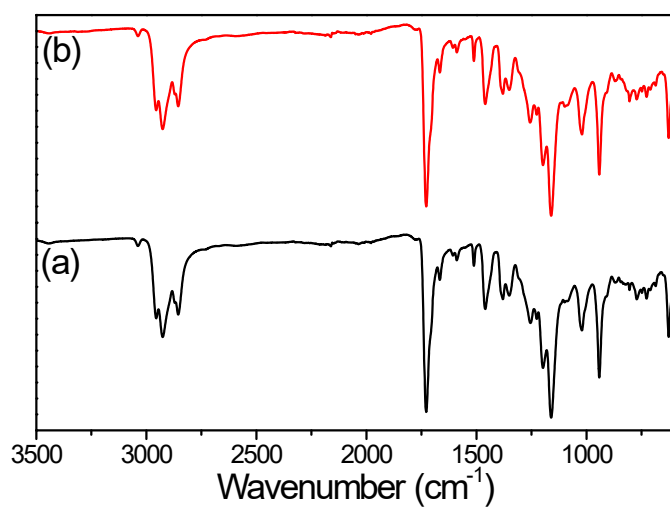


Figure S10. ATR-IR spectra of L -[PTNBP₅-(b -PBHPI₁₀)₂-(b -PEHD₂₀₀)₄] (a) and bicyclic c -[PTNBP₅-(b -PEHD₂₀₀)₄-(b -PBHPI₁₀)₂] (b) measured at 25 °C.

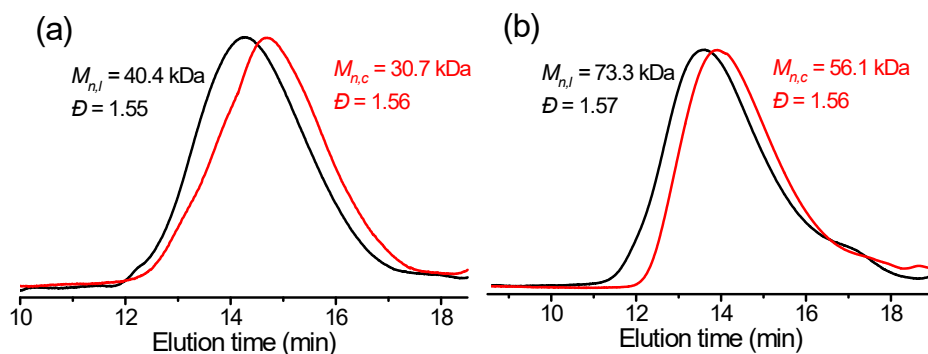


Figure S11. GPC traces of *l*-PBHPI₂₀-(*b*-PEHD_m)₂ and monocyclic *c*-[PBHPI₁₀-(*b*-PEHD_m)₂-(*b*-PBHPI₁₀)] where m=100 (a) and m=200 (b).

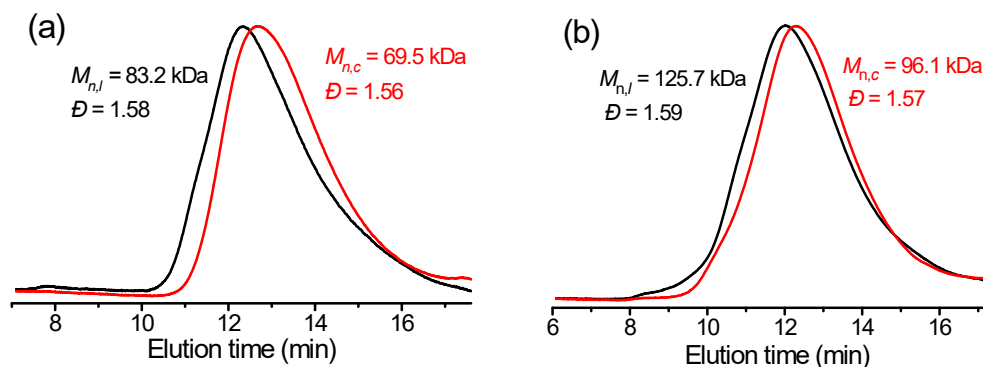


Figure S12. GPC traces of linear *l*-[PTNBP₅-(*b*-PBHPI₁₀)₂-(*b*-PEHD_m)₄] and bicyclic *c*-[PTNBP₅-(*b*-PEHD_m)₄-(*b*-PBHPI₁₀)₂], in which (a) m=100 and (b) m=200.

Table S5 Intrinsic viscosity data over a range of M_w for bicyclic and linear polymers, and $[\eta]_c/[\eta]_l$.

<i>l</i> -[PTNBP ₅ -(<i>b</i> -PBHPI ₁₀) ₂ -(<i>b</i> -EHD ₂₀₀) ₄]		<i>c</i> -[PTNBP ₅ -(<i>b</i> -PEHD ₂₀₀) ₄ -(<i>b</i> -PBHPI ₁₀) ₂]		$[\eta]_c/[\eta]_l$
Log(M_w)	$[\eta]_l$ (mL g ⁻¹)	Log(M_w)	$[\eta]_c$ (mL g ⁻¹)	
5.1	89.7	5.1	75.1	0.83
5.2	101.9	5.2	83.9	0.82
5.3	116.1	5.3	98.0	0.84
5.4	132.3	5.4	114.4	0.86
5.5	156.2	5.5	134.7	0.86
5.6	200.8	5.6	166.1	0.83

Table S6 $\langle R_g \rangle$ values over a range of M_w for bicyclic and linear polymers, and $\langle R_g^2 \rangle_c / \langle R_g^2 \rangle_l$.

<i>l</i> -[PTNBP ₅ -(<i>b</i> -PBHPI ₁₀) ₂ -(<i>b</i> -EHD ₂₀₀) ₄]		<i>c</i> -[PTNBP ₅ -(<i>b</i> -PEHD ₂₀₀) ₄ -(<i>b</i> -PBHPI ₁₀) ₂]		$\langle R_g^2 \rangle_c / \langle R_g^2 \rangle_l$
M_w (Da)	$\langle R_g \rangle$ (nm)	M_w (Da)	$\langle R_g \rangle$ (nm)	
50033	25.62	50095	17.11	0.45
70245	29.19	70362	20.38	0.49
90370	31.87	90404	22.24	0.49
110012	34.21	110135	24.68	0.52

131039	36.29	130141	26.82	0.54
150343	38.61	150648	29.04	0.56
190359	42.76	190574	32.52	0.58
211259	44.67	211813	34.38	0.59
274180	50.76	273771	39.21	0.59
293638	53.05	293832	40.36	0.57
333475	56.67	332773	43.38	0.58
372308	59.24	371775	45.70	0.59
406938	61.87	403247	47.21	0.58
457372	64.47	454296	48.77	0.57

Hydrodynamic volume

The hydrodynamic diameter (D_h) of linear, monocyclic, and bicyclic polymers were determined by dynamic light scattering (DLS) at a concentration of 1 mg mL⁻¹ in THF, and the D_h s values of monocyclic *c*-[PBHPI₁₀-(*b*-PEHD₁₀₀)₂-(*b*-PBHPI₁₀)] and bicyclic *c*-[PTNBP₅-(*b*-PEHD₁₀₀)₄-(*b*-PBHPI₁₀)₂] were 5 nm and 8 nm, respectively (Figures S13a and S13c), which were smaller than those of the corresponding linear *l*-PBHPI₂₀-(*b*-PEHD₁₀₀)₄ (D_h =10 nm) and *l*-[PTNBP₅-(*b*-PBHPI₁₀)₂-(*b*-PEHD₁₀₀)₄] (D_h =15 nm), due to the smaller hydrodynamic volume of cyclic polymers (Table S7). As the increase in PEHD chain length, the D_h s of monocyclic *c*-[PBHPI₁₀-(*b*-PEHD₂₀₀)₂-(*b*-PBHPI₁₀)] (D_h =13 nm) and bicyclic *c*-[PTNBP₅-(*b*-PEHD₂₀₀)₄-(*b*-PBHPI₁₀)₂] (D_h =23 nm) were also smaller than those of linear counterparts *l*-PBHPI₂₀-(*b*-PEHD₂₀₀)₂ (D_h =16 nm) and *l*-[PTNBP₅-(*b*-PBHPI₁₀)₂-(*b*-PEHD₂₀₀)₄] (D_h =28 nm) (Figures S13b and S13d).

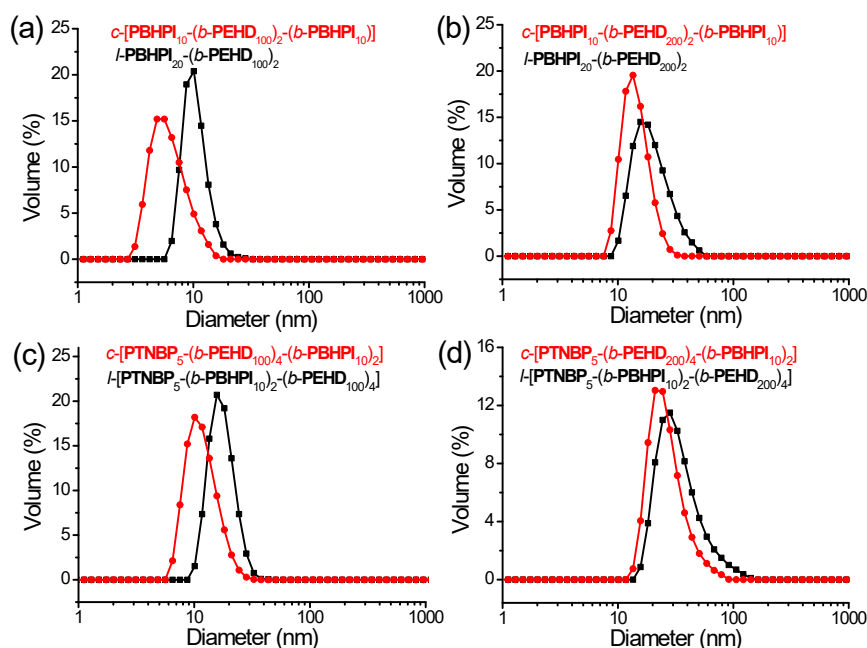


Figure S13. DLS curves of linear and monocyclic (a,b) and linear and bicyclic (c,d) polymers.

Table S7 Characteristic data for linear and cyclic polymers.

Entry	Polymer	D_h (nm) ^a	T_g (°C) ^b	T_d (°C) ^c
1	<i>l</i> -PBHPI ₂₀ -(<i>b</i> -PEHD ₁₀₀) ₂	10	/	/
2	<i>c</i> -[PBHPI ₁₀ -(<i>b</i> -PEHD ₁₀₀) ₂ -(<i>b</i> -PBHPI ₁₀)]	5	/	/
3	<i>l</i> -PBHPI ₂₀ -(<i>b</i> -PEHD ₂₀₀) ₂	16	100	320
4	<i>c</i> -[PBHPI ₁₀ -(<i>b</i> -PEHD ₂₀₀) ₂ -(<i>b</i> -PBHPI ₁₀)]	13	107	337
5	<i>l</i> -[PTNBP ₅ -(<i>b</i> -PBHPI ₁₀) ₂ -(<i>b</i> -PEHD ₁₀₀) ₄]	15	/	/
6	<i>c</i> -[PTNBP ₅ -(<i>b</i> -PEHD ₁₀₀) ₄ -(<i>b</i> -PBHPI ₁₀) ₂]	8	/	/
7	<i>l</i> -[PTNBP ₅ -(<i>b</i> -PBHPI ₁₀) ₂ -(<i>b</i> -PEHD ₂₀₀) ₄]	28	114	339
8	<i>c</i> -[PTNBP ₅ -(<i>b</i> -PEHD ₂₀₀) ₄ -(<i>b</i> -PBHPI ₁₀) ₂]	23	123	339

^aDetermined by DLS. ^bDetermined by DSC. ^cDetermined by TGA.

Thermal properties of cyclic polymers

DSC thermograms for linear *l*-PBHPI₂₀-(*b*-PEHD₂₀₀)₂ and monocyclic *c*-[PBHPI₁₀-(*b*-PEHD₂₀₀)₂-(*b*-PBHPI₁₀)] (Figure S14a), and linear *l*-[PTNBP₅-(*b*-PBHPI₁₀)₂-(*b*-PEHD₂₀₀)₄] and bicyclic *c*-[PTNBP₅-(*b*-PEHD₂₀₀)₄-(*b*-PBHPI₁₀)₂] (Figure S14b) showed that the T_g values of monocyclic and bicyclic polymers were 107 °C and 123 °C, and those of the corresponding linear polymers were 100 °C and 114 °C (Table S7), separately. As expected, both monocyclic and bicyclic polymers behaved a markedly higher T_g than their corresponding linear counterparts with similar molecular weights. Interestingly, the significant difference in T_g of monocyclic *c*-[PBHPI₁₀-(*b*-PEHD₂₀₀)₂-(*b*-PBHPI₁₀)] and bicyclic *c*-[PTNBP₅-(*b*-PEHD₂₀₀)₄-(*b*-PBHPI₁₀)₂] was also presented, which was depended on the molecular weight and ring number of cyclic polymers, and the T_g values

converge at high molecular weight. In addition, linear l -PBHPI₂₀-(b -PEHD₂₀₀)₂, monocyclic c -[PBHPI₁₀-(b -PEHD₂₀₀)₂-(b -PBHPI₁₀)], linear l -[PTNBP₅-(b -PBHPI₁₀)₂-(b -PEHD₂₀₀)₄], and bicyclic c -[PTNBP₅-(b -PEHD₁₀₀)₄-(b -PBHPI₁₀)₂] exhibited highly thermal stability with the T_d values of 320 °C, 337 °C, 339 °C, and 339 °C (Figure S15, and Table S7), respectively, while the T_d of classic PA was lowered to about 200 °C.

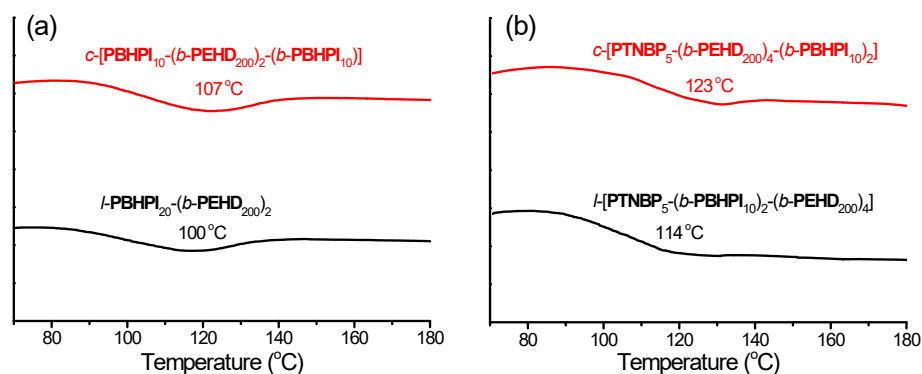


Figure S14. DSC curves of linear vs monocyclic polymers (a) and linear vs bicyclic polymers (b) in the second heating process.

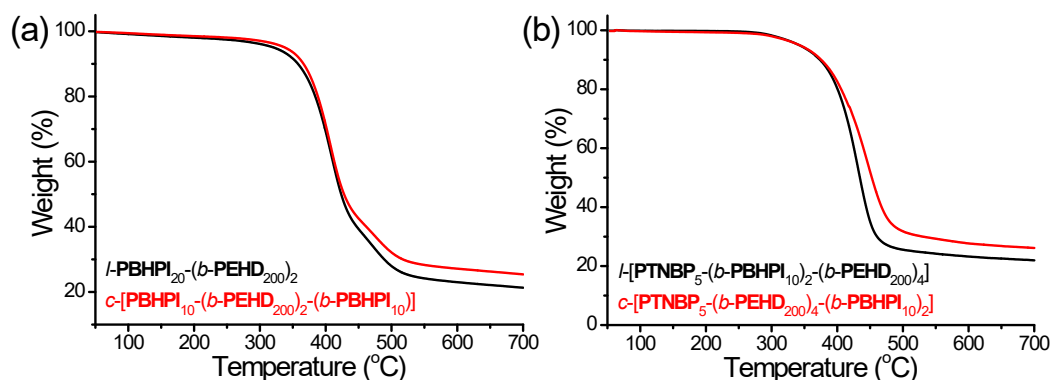


Figure S15. TGA curves of linear and monocyclic polymers (a), and linear and bicyclic polymers (b).

Photoelectric properties of cyclic polymers

The photophysical properties of polymers were evaluated by UV-vis absorption in solution and thin film state. The UV-vis spectra with two well-resolved absorption peaks at 500-600 nm in solution (Figure S16). In addition, the absorption strength of monocyclic and bicyclic polymers was weaker than that of the corresponding linear polymers, and as extending the chain length of PEHD, the absorption strength also increased. As the constraint of cyclic topology, the strong π - π stacking interaction of all-trans PA segments resulted in a reduced absorption strength of cyclic polymer. Furthermore, the bandgap (E_g) values of linear l -PBHPI₂₀-(b -PEHD₂₀₀)₂ and l -[PTNBP₅-(b -PBHPI₁₀)₂-(b -PEHD₂₀₀)₄], and the corresponding monocyclic c -[PBHPI₁₀-(b -PEHD₂₀₀)₂-(b -PBHPI₁₀)] and bicyclic c -[PTNBP₅-(b -PEHD₂₀₀)₄-(b -PBHPI₁₀)₂] were 1.85, 1.82, 1.83, and 1.81 eV, respectively,

which were calculated by the onset absorption of polymers in solution according to the formula of $E_g=1240/\lambda_{\text{edg}}$. The λ_{edg} of tetrafunctional monomer **TNBP** and difunctional monomer **BHPI** were appeared at 441 nm and 558 nm (Figure S17), respectively, while the λ_{edg} for cyclic or linear polymer was all larger than 700 nm, which is more likely due to the influence of PA skeleton rather than the pyrene or perylene unit. Interestingly, the maximum absorption profiles of *l*-**PBHPI**₂₀-(*b*-**PEHD**₂₀₀)₂, monocyclic *c*-[**PBHPI**₁₀-(*b*-**PEHD**₂₀₀)₂-(*b*-**PBHPI**₁₀)], *l*-[**PTNBP**₅-(*b*-**PBHPI**₁₀)₂-(*b*-**PEHD**₂₀₀)₄], and bicyclic *c*-[**PTNBP**₅-(*b*-**PEHD**₂₀₀)₄-(*b*-**PBHPI**₁₀)₂] in the free-standing film state have changed from two distinct peaks to a broader single peak, and the overall absorption intensity was enhanced obviously, which was conducive to improving electron mobility. Besides, the onset absorption wavelength for linear *l*-**PBHPI**₂₀-(*b*-**PEHD**₂₀₀)₂, monocyclic *c*-[**PBHPI**₁₀-(*b*-**PEHD**₂₀₀)₂-(*b*-**PBHPI**₁₀)], linear *l*-[**PTNBP**₅-(*b*-**PBHPI**₁₀)₂-(*b*-**PEHD**₂₀₀)₄], and bicyclic *c*-[**PTNBP**₅-(*b*-**PEHD**₂₀₀)₄-(*b*-**PBHPI**₁₀)₂] extended to 726, 715, 760, and 739 nm (Figure 3a, Table S8) with the E_g narrowed to 1.70 eV, 1.73 eV, 1.63 eV, and 1.67 eV, respectively, which possessed broad application prospects in the field of solar cells as the non-fullerene acceptor materials.

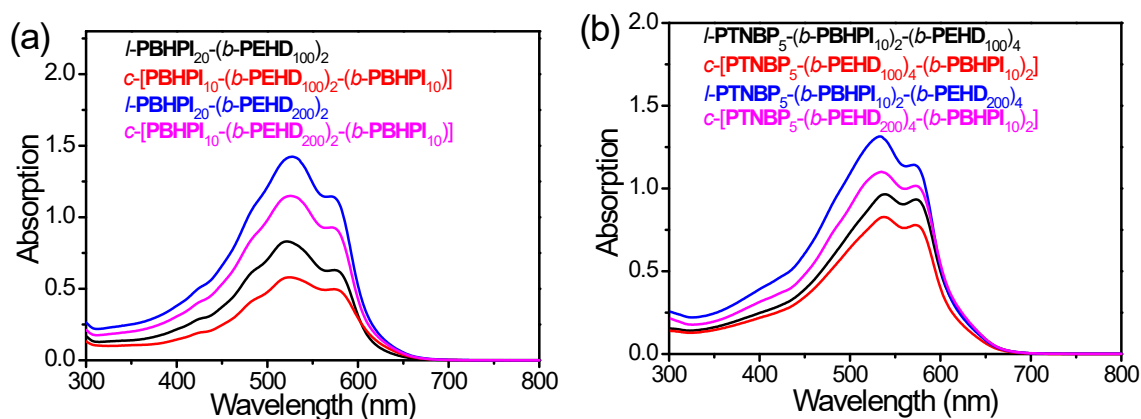


Figure S16. UV-vis spectra of linear and monocyclic polymers (a), and linear and bicyclic polymers (b) at 0.03 mg mL⁻¹ in THF solution.

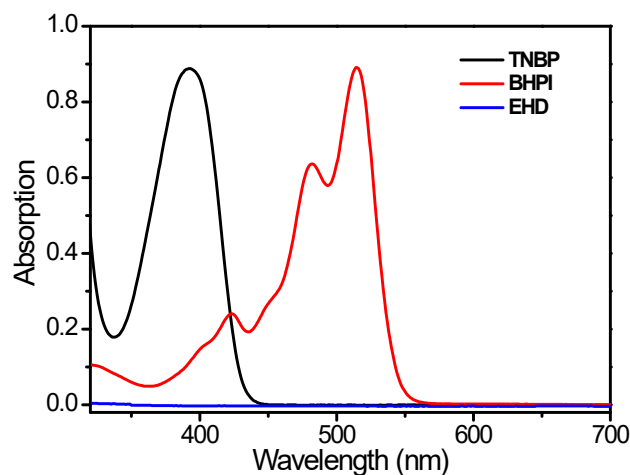


Figure S17. UV-vis spectra of tetrafunctional monomer **TNBP** (black), difunctional monomer **BHPI** (red), and monofunctional monomer **EHD** (blue) in THF solution at 0.03 mg mL⁻¹.

To eliminate the effect of concentration on the absorbance, the UV-vis analysis of bicyclic polymer and its linear analogs was conducted for comparison the absorption intensity of polymers at different concentrations, and the extinction coefficients (ϵ) were calculated to be 35.49 and 36.33 (Fig. S18, ESI[†]), respectively, meaning that the difference in absorption intensity of polymers was caused by the different topology rather than the concentration.

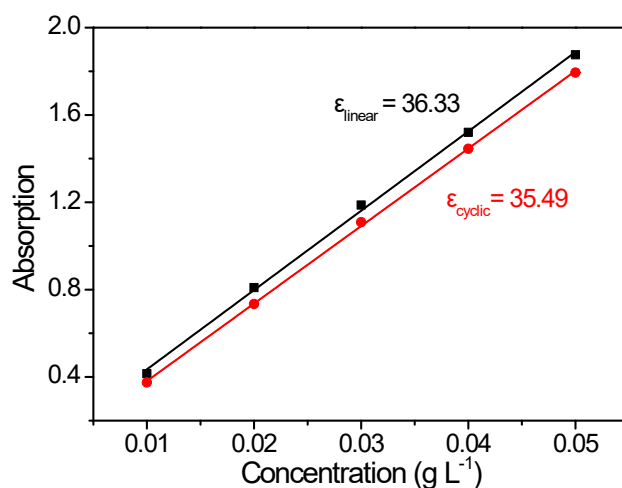


Figure S18. The extinction coefficient (ϵ) of linear *l*-[PTNBP₅-(*b*-PBHPI₁₀)₂-(*b*-PEHD₂₀₀)₄] (black) and bicyclic *c*-[PTNBP₅-(*b*-PEHD₂₀₀)₄-(*b*-PBHPI₁₀)₂] (red) from UV-vis spectra (the ϵ was calculated according to the formula $A = \epsilon bc$, where A is the absorbance intensity, ϵ is the extinction coefficient, b is the optical path of the cuvette, and c is the concentration of the light absorbing substance).

Table S8 Photoelectric properties of polymers.

Polymer	E_g (eV) ^a	λ_{edg} (nm) ^b	E_g (eV) ^c	$E_{\text{onset}}^{\text{red}}$ (V) ^d	E_{HOMO} (eV) ^e	E_{LUMO} (eV) ^f
<i>l</i> -PBHPI ₂₀ -(<i>b</i> -PEHD ₂₀₀) ₂	1.85	726	1.70	-0.33	-5.77	-4.07

<i>c</i> -[PBHPI ₁₀ -(<i>b</i> -PEHD ₂₀₀) ₂ -(<i>b</i> -PBHPI ₁₀)]	1.83	715	1.73	-0.28	-5.85	-4.12
<i>l</i> -[PTNBP ₅ -(<i>b</i> -PBHPI ₁₀) ₂ -(<i>b</i> -PEHD ₂₀₀) ₄]	1.82	760	1.63	-0.31	-5.72	-4.09
<i>c</i> -[PTNBP ₅ -(<i>b</i> -PEHD ₂₀₀) ₄ -(<i>b</i> -PBHPI ₁₀) ₂]	1.81	739	1.67	-0.29	-5.78	-4.11

^aIn solution. ^bIn film state. ^cIn film state, $E_g=1240/\lambda_{\text{edg}}$. ^dThe onset reduction potential determined by CV. ^e $E_{\text{LUMO}}=-(4.4+E_{\text{onset}}^{\text{red}})$. ^f $E_{\text{HOMO}}=E_{\text{LUMO}}-E_g$.

References

- 1 W. Song, H. J. Han, J. H. Wu, M. R. Xie, *Chem. Commun.*, 2014, **50**, 12899-12902.
- 2 J. Chen, R. Y. Sun, X. J. Liao, H. J. Han, Y. W. Li, M. R. Xie, *Macromolecules*, 2018, **51**, 10202-10213.
- 3 J. A. Love, J. P. Morgan, T. M. Trnka, R. H. Grubbs, *Angew. Chem. Int. Ed.*, 2002, **41**, 4035-4037.
- 4 J. Chen, D. Zhou, C. Wang, X. Liao, M. Xie, R. Sun, *RSC Adv.*, 2016, **6**, 88874-88885.